ELSEVIER

Polymer 44 (2003) 1661–1669

polymer

www.elsevier.com/locate/polymer

Structuring polymer blends with bicontinuous phase morphology. Part II. Tailoring blends with ultralow critical volume fraction

J. Lyngaae-Jørgensen[a,*], L.A. Utracki[b]

[a]Department of Chemical Engineering, Building 229, Technical University of Denmark, DTU, DK-2800 Kgs. Lyngby, Denmark
[b]National Research Council Canada, IMI, Boucherville, Que., Canada

Abstract

A hypothesis providing a guideline for the development of immiscible polymer blends with co-continuous phase structure at very low critical volume fraction of one component is postulated and experimentally verified. Based on a number of simplifying assumptions the following relation was derived: $\phi_{cr} = k(\lambda\dot{\gamma})^{1-z}/(\theta_b^*)^z$ where $\lambda\dot{\gamma}$ is a Deborah number and θ_b^* is a dimensionless break-up time. The equation parameters, k and z are constant that depend on the flow field hence on the blending equipment. For the studies an internal mixer with Walzenkneter-type 30 mixing shafts was used. For this equipment the experimental values of the equation parameters, $k = 1801$ and $z = 2.01$, were found.

Keywords: Polymer blends; Bicontinuous phase structure; Ultralow critical volume fraction

1. Introduction

Most properties of immiscible polymer blends depend on the morphology or the two-phase structure [1]. There is a great diversity of immiscible polymer blends morphology, but, from the point of view of the performance, they may be divided into two categories: (1) blends with discrete phase structure (DPS, or drop-in matrix), and (2) blends with bicontinuous phase structures (BPS, or co-continuous). In the latter case, phases A and B form co-continuous, interpenetrating structures, which Sperling and his co-workers labeled a ‘thermoplastic IPN’ [2]. In BPS, when the correlation length of the phase structure is much smaller than a minimum characteristic sample length, universal relationships can be found for a series of properties (e.g. elastic modulus, electrical conductivity, permeability, etc.). These may be cast in a form of the ‘power-law’ expression: $P - P_{cr} \propto (\phi - \phi_{cr})^x$, where P is a property, e.g. a modulus or electrical conductivity, P_{cr} is the value of P at the critical volume fraction, x is a universal exponent, ϕ is the volume fraction of one blend component and ϕ_{cr} is its threshold volume fraction (critical volume fraction) for the formation of infinite bicontinuous structure [3,4].

As early as in 1967, Starita [5] found that mixing polystyrene (PS) with a small amount of polyethylene (PE) in an elastic melt extruder (EME) could lead to formation of a co-continuous structure. In 1980, Thornton et al. [6] wrote that “if PS and PE are melt blended in an EME and the extrudate is then immersed in toluene, the PS is solution extracted leaving behind the PE in a form that somewhat resembles an open-cell foam, indicating that the PS was a continuous phase in the open cells of the PE. This two-phase interpenetrating network morphology has been found even in extreme cases, such as when 1% PE is blended with 99% PS and when the PS is solvent extracted a fine, three-dimensional (3D) cobweb of PE remains”.

A number of other publications reported BPS in PE/PS blends [7–13]. For example, Fayt et al. [7] stated that: “The PE network formed during melt processing is rapidly disrupted into dispersed particles upon heating the blends at 200 °C for only a few minutes”. The same group has been studying the stabilizing effects of addition of diblock copolymers to these blends [8].

Several papers have considered the so-called phase inversion phenomenon and its prediction. For low viscosity A/B mixtures, e.g. A/B = oil/water, one observes that at low volume fraction of A discrete drops of A are formed in a continuum of B. When the volume fraction of A is gradually increased, at a critical phase inversion volume fraction a co-continuity may be found, then the structure changes to B

Abbreviations: BPS, bicontinuous phase structure; HDPE, high density polyethylene; PDMS, polydimethylsiloxane; PS, polystyrene; THF, tetrahydrofuran.

[*] Corresponding author.

0032-3861/03/$ - see front matter © 2002 Elsevier Science Ltd. All rights reserved.
PII: S0032-3861(02)00867-4

Nomenclature

a	characteristic dimension
k, k_1, k_2, k_3	constants
p	aspect ratio
P	coagulation probability
t_c	contact time
x	exponent in Eq. (2)
z	exponent in Eq. (8)
$\dot{\gamma}$	shear rate
η_A	viscosity of phase A
η_B	viscosity of phase B
η_D	viscosity of dispersed (minor) phase
η_C	viscosity of continuous (major) phase
θ_c	time of coagulation
θ_b	break-up time
θ_b^*	dimensionless break up time
θ_d^*	dimensionless equilibrium deformation time
κ	capillarity number
κ^*	reduced capillarity number
κ_{cr}	critical value of capillarity number
λ^*	viscosity ratio (η_D/η_C)
λ	characteristic time
ν	interfacial tension coefficient
σ_{12}	shear stress
ϕ	volume fraction
ϕ_{cr}	critical volume fraction for BPS formation
$\Phi_{I,A}$	continuity index of phase A: volume fraction of polymer A being a part of BPS
$\Phi_{I,B}$	continuity index of phase B

drops being dispersed in A matrix. Thus, in the mixtures of Newtonian liquids the phase inversion takes place over a narrow range of volume fraction leading to unambiguous determination of ϕ_{cr}. By contrast, in polymer blends the phase inversion occurs over a rather broad interval, with bicontinuous phase separating the two DPS regions [14–19].

In the description of the bicontinuous structure, a 'co-continuity mapping' may be helpful. The term, coined by Utracki [20], defines the volume fractions of A and B within the phase inversion region: $\Phi_{I,A}, \Phi_{I,B} \to 1$, where the co-continuity index of A is $\Phi_{I,A}$ and co-continuity index of B is $\Phi_{I,B}$, as shown in Fig. 1. In other words, within the phase inversion region of blend compositions all polymer A and all polymer B may participate in co-continuous structures and the volume fraction of the DPS is identical to zero: $\Phi_{DPS} \equiv 0$.

Recently, Steinmann et al. examined the phase inversion theories [21]. The authors had concluded that a modified version of a theory published by Utracki [20] offers the best description of data. The authors defined the phase inversion volume fraction, ϕ_{2I}, by the minimum when plotting a form factor vs. volume fraction. This may be considered an alternative, operational definition of ϕ_{2I}.

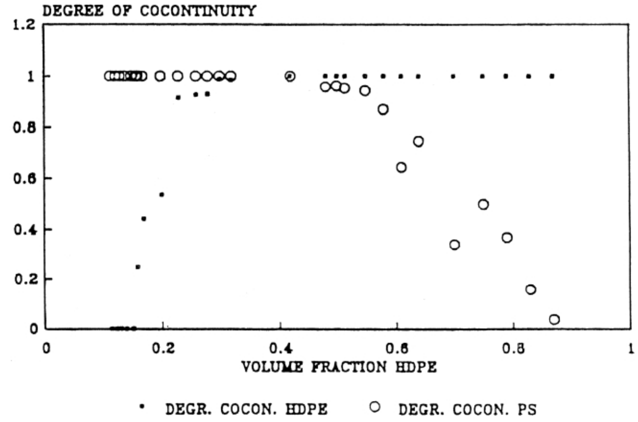

Fig. 1. Degree of co-continuity as a function of the volume fraction for HDPE-1 in its blends with PS (Polysor, Polystyrene-210, η_0(180 °C) = 25 kPa) [14].

Utracki's derivation [20] is based on the assumption that in a mixture of two immiscible liquids (treated as 'emulsion of A in B and that of B in A'), at a specific composition: $\phi_{2I} = 1 - \phi_{1I}$, the flow behavior is the same, independent whether one starts with diluting liquid-1 with liquid-2 or vice-versa. Thus, equating the constant stress viscosities of the two polymer blends, $\eta_1 = \eta_2$, where the shear viscosity η_i is taken at σ_{12} = constant, leads to a simple predictive dependence:

$$\eta_1/\eta_2 = [(\phi_m - \phi_{2I})/(\phi_m - \phi_{1I})]^{[\eta]\phi_m} \quad (1)$$

The condition: $\phi_{2I} = \phi_{1I} = 1$ defines the phase-inversion volume fraction, where the two co-continuity curves in Fig. 1 cross. The other volume fraction parameter, $\phi_m \simeq 1 - \phi_{perc}$ is the classical 'maximum packing volume fraction' in relative viscosity description of the two-phase flows. For emulsions its value is related to the percolation threshold volume fraction, ϕ_{perc}, which in turn depends on the type of flow—for random 3D mixing the theory predicts that $\phi_{perc} \cong 0.156$ while for uniaxial stretching flows in 1D its value is about eight times smaller: $\phi_{perc} = 0.019$. The last quantity in the relation, the intrinsic viscosity $[\eta]$, is a measure of the hydrodynamic volume of the dispersed phase. According to Oldroyd, for the emulsions its value ranges from 1 to 2.5, depending on several viscosity ratios, specified by the theory [22,23]. It is noteworthy that during flow of a immiscible binary blend the constant velocity gradient is discontinuous at the interphase—only the stress is continuous across the interface, thus for the multiphase system, the persistent use of the viscosity vs. rate of deformation plots is fundamentally wrong.

Relatively few papers deal with the volume fraction interval, where the bicontinuous phases can be found [14–19]. Lyngaae-Jørgensen et al. [15] assumed that co-continuous structures might be formed as a result of a break-up and coalescence processes. The authors tried to predict the formation of infinite structures considering the number of contacts between domains and the probability that while in direct contact they would develop strong links one to another that result in coalescence. Posthuma de Boer and co-workers [16–18,24] developed a theory predicting a concentration range where fully bicontinuous structures may be expected (in the nomenclature used in the present paper, this is the interval where both phase A and phase B are co-continuous, i.e. $\Phi_{I,A} = \Phi_{I,B} = 1$).

A necessary condition for the formation of a co-continuous structure is that the rate of coagulation is non-zero. In analogy to Elmendorp's [25] nomenclature, we call this case Region II, (in contrast with Region I where the rate of coalescence = 0). Elmendorp considered the case of two Newtonian drops contacting each other in a simple shear flow field, thus at infinite dilution. A more general theory has not been developed, but Region II may be defined as one where, for a random 3D flow of well-dispersed immiscible polymer blends, the rate of coalescence ≠ 0. It may take a long time for a polymer blend to reach an invariant structure during flow.

Considering the ephemeral phase co-continuity for Newtonian systems, one may argue that the wide range of volume fractions, where the bicontinuous phase morphologies are observed in polymer blends, represent a transient state—had the shearing continued for longer period the structures would disintegrated into DPS. Owing to thermal stability of polymers in the molten state, one may not be able to refute such an argument by experiments. However, during the present studies, some blends with dual phase morphology under steady-state flow remained stable for hours.

The purpose of the present work is to elucidate the formation of BPS in blends with low critical volume fraction, and to predict the conditions for formation of such bicontinuous structure.

2. Hypothesis

According to the percolation theory a bicontinuous-phase structure (BPS) can be created in a finely dispersed immiscible polymer blend, when the volume fraction of the minor component exceeds a critical value, ϕ_{cr} [15]:

$$\phi_{cr} \simeq Kp^{-x} \tag{2}$$

In Eq. (2): K is an equation constant, p is the aspect ratio of dispersed particles and x is a power-law exponent with value between 1 and 2. For blends with the aspect ratio close to 1 (nearly spherical drops) K-value was found to be numerically nearly identical to $\phi_{cr} = 0.156$ in 3D [15]. Thus, for spherical 'precursors' in strictly immiscible blends the critical volume fraction at which the BPS starts percolating throughout the whole sample is $\phi_{cr} \cong 0.16$. The expression assumes that a close contact between two domains causes a strong link to form between them.

Starting from infinite dilution and increasing the volume fraction of minor phase the necessary and critical conditions under which a BPS are first formed are: (1) long fibers with the largest possible aspect ratio are formed (Eq. (2)), and (2) the fibers coagulate before they break up. Consequently the lowest critical volume fraction will be found when at constant stress the diameter of a domain is as small as possible. To find a BPS structure in the final product the fibers must form a network. This is achieved when the break-up time is longer than that for coagulation and a BPS structure survives the treatments it receives after it is formed.

It is postulated that if the time for coagulation (θ_c) of two contacting long ellipsoidal domains (nearly cylindrical, or of an arbitrary spaghetti-like shape) are smaller than or equal to the time to break of a cylindrical liquid domain (θ_b), $\theta_c \leq \theta_b$, a BPS may form. Consequently, (for Regime II, $\sim 1 < \eta_D/\eta_C \leq 3.8$; $\phi_{cr} \leq 0.16$ and for shear-dominated flows, $\dot{\gamma} \gg \dot{\varepsilon}$, $\dot{\gamma} > \dot{\gamma}_{cr}$) the critical condition for BPS formation is:

$$\theta_c = \theta_b \tag{3}$$

As shown in Fig. 2 of Ref. [26], the normalized break-up time θ_b^* depends on the viscosity ratio $\lambda^* \equiv \eta_D/\eta_C$ (η_D and η_C is the viscosity of the dispersed and continuous phase, respectively). The normalization was:

$$\theta_b^* \equiv \theta_b \dot{\gamma}/\kappa = \theta_b(\nu\dot{\gamma}/\sigma_{12}a) \tag{4}$$

The capillarity number: $\kappa \equiv \sigma_{12}a/\nu$, where σ_{12} is the shear stress, a is a characteristic dimension, ν is the interfacial tension coefficient and $\dot{\gamma}$ is the shear rate. Analysis of experimental data published by Grace, and by Elemans indicated a simple dependence: $\theta_b^* = 99.31(\lambda^*)^{0.355}$; $1 \leq \lambda^* \leq 3.8$ [26].

The time to coalescence should be proportional to the contact time, t_c, and the coagulation probability, P:

$$\theta_c \propto t_c P \tag{5}$$

For a spaghetti-like domain in contact with another spaghetti-like domain t_c may be written as $(p/\dot{\gamma})$. The probability of coagulation, P, scales with $(p/\lambda\dot{\gamma})$, where λ is

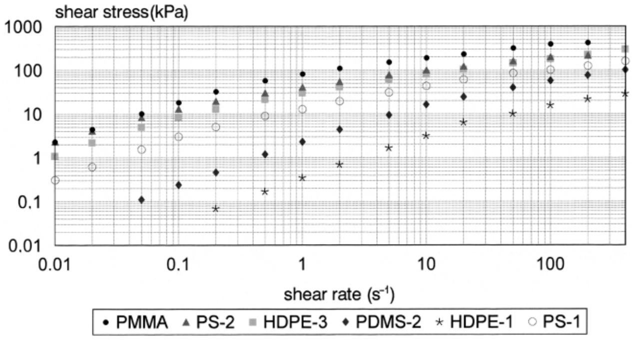

Fig. 2. Flow curves at 180 °C as measured shear stress for a set value of shear rate.

a characteristic time constant. Thus, from Eqs. (3)–(5): $\theta_c \propto (p/\dot{\gamma})(p/\lambda\dot{\gamma}) \propto \theta_b^*(\kappa/\dot{\gamma})$, or

$$p^2 = k_1\theta_b^*(\lambda\dot{\gamma})\kappa \tag{6}$$

where k_1 is the proportionality factor. When blending is carried out in dilute systems, the capillary number, κ, at or near steady state in simple shear flow ($\lambda^* <$ critical value) and extensional flow slowly varies with λ^* [25,26]. Consequently Eq. (6) simplifies further by absorbing κ into k_1. Thus, Eq. (6) predicts that the aspect ratio of deformed particles at the dynamic equilibrium ($\theta_c = \theta_b$) is nearly independent of viscosity ratio [$p \propto (\lambda^*)^{0.177}$] and proportional to the square root of the deforming energy [$p \propto \sqrt{\sigma_{12}\dot{\gamma}}$].

From Eq. (2) the critical condition for BPS formation may be expressed as: $k_2\phi_{cr}p^xP \equiv 1$, or $k_2\phi_{cr}p^{x+1}/\lambda\dot{\gamma} = 1$, where k_2 is another constant. Incorporation of p from Eq. (6) leads to:

$$\phi_{cr} = k(\lambda\dot{\gamma})(\theta_b^*\lambda\dot{\gamma})^{-x+1/2} \tag{7}$$

where $k =$ constant. Finally, re-defining a new exponent: $z = (x+1)/2$, the critical condition for BPS formation in Regime II may be written as:

$$\phi_{cr} = k(\theta_b^*)^{-z}(\lambda\dot{\gamma})^{1-z} \tag{8}$$

The necessary condition for the expression given in Eq. (8) is that a drop is deformed to fiber-like structures before it breaks into small droplets.

The microrheology has been formulated for the infinitely diluted mixtures of Newtonian liquids. It defines the conditions for fiber formation and break-up in terms of the viscosity ratio, ($\lambda^* \equiv \eta_D/\eta_C$, the reduced capillary number, $\kappa^* \equiv \kappa/\kappa_{cr} = (\sigma_{ij}a/\nu)/\kappa_{cr}$, and reduced time, $\theta^* \equiv \theta\dot{\gamma}/\kappa$, where κ_{cr} is a critical value. From the point of view of drop deformation and break there are four regions of the reduced capillary numbers κ^* [26]:

for $0.1 > \kappa^*$ droplets do not deform,
for $0.1 < \kappa^* < 1$ droplets deform, but they do not break,
for $1 < \kappa^* < 2$ droplets deform then split into two primary droplets,
for $\kappa^* > 2$ droplets deform into stable filaments.

Thus, for $\kappa^* > 2$, drops of the minor phase deform affinely with the matrix into long fibers and the phase co-continuity is obtained. When subsequently the deforming stress decreases, causing κ^* to fall below 2, the fiber disintegrates under the influence of the capillary instability. The co-continuous structure has been observed for mixtures of Newtonian liquids in Couette geometry, suggesting that formation of BPS is a general phenomenon, related to stress (thus, to coalescence and break-up time interrelation) and not to viscoelasticity.

Similarly as with κ^*, the drop deformability also depends on the viscosity ratio $\lambda^* \equiv \eta_D/\eta_C$ and the break-up time, θ_b^*. When values of κ^* and θ^* are within the range required for drop break up, the mechanism of rupture depends on λ^*. In shear four regions have been identified:

for $0.1 \gg \lambda^*$ small droplets are shed from sigmoidal drops—tip spinning,
for $0.1 < \lambda^* < 1$ drop breaks into two principal and odd number of satellite droplets,
for $1 < \lambda^* < 3.8$ drop deforms into fiber, which then disintegrate into small droplets,
for $\lambda^* > 3.8$ drops deform, but they do not break.

The microrheology also specifies the reduced time scale for the equilibrium deformation (θ_d^*) and for break-up of fibers when κ^* falls below 2, $\theta_d^* = 25$ and $\theta_b^*(\lambda^*) \leq 160$, respectively.

The microrheology gives a simple prescription for developing co-continuity of phases in Newtonian systems: $\kappa^* > 2$, $1 < \lambda^* < 3.8$, and $\theta_d^* \geq 25$. In others than Couette geometry, these conditions may not guarantee the BPS formation in infinitely diluted blends.

3. Experimental

3.1. Materials

Series of blends of two commercial PS with three high density polyethylenes (HDPE), two polydimethyl siloxanes (PDMS) and polymethylmethacrylate (PMMA) were prepared. The materials characteristic is given in Tables 1 and 2. The steady state shear flow behavior of these resins at 180 °C was determined using Rheometrics RDII in the parallel plates geometry (low shear rates) and in Rosand capillary rheometer (high shear rates). The flow curves in a form of shear stress vs. shear rate for these (neat) polymers are shown in Fig. 2.

3.2. Blend preparation

The blend constituents were dried in a vacuum oven at 50–60 °C for a week. The blending was carried out in a Brabender Plasticorder (chamber volume of ca. 33 ml and a Walzerkneter Type 30 mixing shafts) at 180 °C and 20 rpm for 15–20 min. After mixing, the chamber was opened and the sample was air-cooled. For solvent extractions the specimens were cut from the cooled blend into a well-defined shape, or alternatively they were molded into 1 or 2 mm thick sheets using a hydraulic press at 200 °C. The influence of mixing time and rotation speed on the bi-continuity index were studied for PS blended with 2.2 or 10 vol% HDPE-3.

The measurements using scanning electron microscope (SEM), size exclusion chromatography (SEC) and rheometry were carried out according to well-described procedures [14].

Table 1
Characterization of high density polyethylene (HDPE) samples

	Sample				
	HDPE-1	HDPE-2	HDPE-3	HDPE-4	PMMA
Manufacturer	Neste	Neste	Neste	Borealis	Röhm & Haas
Grade	DMDS 7028	DMDS 7007	DMDS 3415	Daplen MS6591	V920-100
ρ (kg/m^3)	960	964	958	961–965	1190
MFI	28	7	0.1		
$\bar{M}_w$ (kg/mol)	60	97	320		89.2
$\bar{M}_n$ (kg/mol)	7.1	11.6	29		44.6
$\bar{M}_w/\bar{M}_n$	8.5	8.4	10.9		2.0
η_0 (kPa s)	0.350	1.9	110	2.7	220

ρ = density; MFI = melt flow index ISO 1133 conditions 4;(g/10 min); η_0 = viscosity at $T = 180$ °C; the molecular weights of HDPE were determined by high temperature SEC; antioxidant: Irganox 1010 (0.1 wt%) used in all HDPE formulations. The standard deviation for $\bar{M}_w$ is ±3%.

3.3. Solvent extraction

These tests quantified the degree of phase co-continuity for the blend. It was immediately evident whether the insoluble component was self-supporting after extraction or not. The following selective solvents were used:

- For PS in PS/HDPE blends: tetrahydrofuran (THF) and as a θ-solvent cyclohexane at 40 °C.
- For PMMA/PS blends formic acid as a solvent for PMMA and cyclohexane at 40 °C for PS.
- For PMMA in PMMA/HDPE blends formic acid and THF.
- For PDMS hexane at room temperature.

The extraction procedure was repeated several times to constant weight of the resulting carcass.

The continuity index, Φ_i, has been defined as the volume fraction of polymer i that is incorporated into an infinite structure, relative to the total volume of that polymer in the sample. Its value for PS was determined as the volume of PS extracted from a specimen divided by the total PS volume in it. For HDPE Φ_i was determined as the amount of PE in a self-supporting cube after extraction, divided by the total amount of PE in the cube. In some HDPE blends with small volume fractions of HDPE (e.g. ≤6 vol%) the samples were swollen in a selective solvent for the other blend component. After drying the swollen sample collapsed, but remain in one coherent piece with weight w_1. The continuity index was defined as w_1 divided by the total HDPE content in the sample.

Table 2
Characteristics of other polymers than HDPE

	Polymer			
	PS-1	PS-2	PDMS-1	PDMS-2
Supplier	Shell	Shell	Bayer	Dow Corning
Grade/type	N 3000	N 7000	M 1000000	SGM-IIL
Density (kg/m^3)	1040	1040	970	970
$\bar{M}_w$ (kg/mol)	283		207.0	600
$\bar{M}_n$ (kg/mol)	108.8		103.6	331.5
$\bar{M}_w/\bar{M}_n$	2.6	3.3	2.0	1.8
η_0 (kPa s), 180 °C	33	300	0.1	2.45
η_0 (kPa s), 200 °C				2.2

ρ = density; MFI = melt flow index ISO 1133 conditions 4;(g/10 min); η_0 = viscosity at $T = 180$ °C; the molecular weights of HDPE were determined by high temperature SEC; antioxidant: Irganox 1010 (0.1 wt%) used in all HDPE formulations. The standard deviation for $\bar{M}_w$ is ±3%.

3.4. Rheometry

To characterize the neat polymers two instruments were used at $T = 180$ °C. For the low deformation rates a Rheometrics RDII with a parallel plates tooling was used in a steady state deformation mode. For the high deformation rates a Rosand double bore capillary rheometer was employed.

4. Results

As reported earlier (see Fig. 1), blends of PS-1 with either HDPE-1 or HDPE-2 had a relatively symmetrical co-continuity index map with full 100% BPS of both phases limited to a narrow range of composition in the vicinity of $\phi_{\mathrm{HDPE}} \cong 0.42$ [4,14]. By contrast, for PS-1/HDPE-3 blends, in Fig. 3 100% BPS of both phases is observed for a wide range of compositions, from $\phi_{\mathrm{HDPE}} \cong 0.02–0.67$.

More precisely, samples of PS-1/HDPE-3 with a volume fraction of 0.5 vol% after extraction with either THF or cyclohexane collapsed into a powder, thus showing DPS morphology. However, when the HDPE-3 content increased to 1.4 and 2 vol%, HDPE swelled during extraction, but it remained coherent thereafter. Thus, for this blend the minimum volume fraction of the high viscosity component in co-continuous blend is: $0.005 \leq \phi_{\mathrm{cr}} \leq 0.014$. When the HDPE-3content increased to about 6 vol%, the specimen placed in THF swelled a little—the volume increased, but the specimen remained in one piece. After extraction of the PS-phase was completed the sample contracted to the final

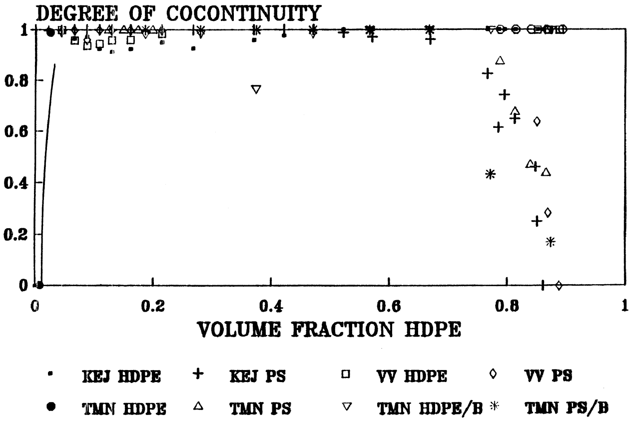

Fig. 3. Co-continuity index for HDPE-3 in its blends with PS-1: $\phi_{i,\mathrm{HDPE3}}$ and $\phi_{i,\mathrm{PS}}$ as function of volume fraction of HDPE-3. (The different symbols are for data measured by different operators.)

coherent, single piece, which then was dried to a constant weight. Samples with HDPE-3 volume fraction: $\phi_{\mathrm{HDPE}} \geq 6$ vol% after extraction kept their original shape (i.e. that of a cube). The swelling kinetics and the amount of swelling were different in THF at room temperature than that in cyclohexane at 40 °C. In the latter case the form changes were smaller but the determined value of ϕ_{cr} was not significant different.

An example of the internal structure of extracted HDPE-3/PS-1 = 10/90 specimen is shown in Fig. 4. Here the fractured surface, observed under SEM, shows extensive fibrillation of the remaining HDPE-3 phase.

During the extraction of HDPE-3/PMMA blends with formic acid the specimen did not change shape.

The influence of composition, mixing shafts rotation speed and the mixing time on the development of co-continuous morphology were studied using the HDPE-3/PS-1 model blends. Results of these tests are shown in Table 3. Mixing was carried out at $T = 180$ °C in an internal mixer, varying the mixing shafts rate of rotation from 5 to 120 rpm, what roughly corresponds to the volume-average value of shear rates: $\dot{\gamma} \approx 4-100\ \mathrm{s}^{-1}$, respectively. Mixing time, $t = 15-120$ min was used and the shafts rotational speed was $N = 5$, 20, 50, 80, and 120 rpm.

Fig. 4. SEM micrograph of a fractured surface of the HDPE-3/PS-1 = 10/90 blend, after PS extraction.

As expected, the blend composition strongly affected the final morphology. Thus, for blends containing 10 vol% HDPE-3 stable BPS morphology was observed for the full range of processing conditions, viz. rate of rotation $N = 5-120$ rpm, or mixing time up to 2 h. (longer mixing time was avoided for fear of thermal degradation since earlier investigations of PS and HDPE samples have shown significant changes in molecular weight distribution at times longer than ca. 2 h at 180 °C). Significantly different behavior was observed for blends with 2.2 vol% HDPE-3. The results are summarized in Table 3. Thus, high degree of co-continuity (~100%) was observed for blends compounded under relatively mild mixing conditions (time and shaft speed), but low at the limiting low and high values.

Evidently, 2.2 vol% HDPE-3 is close to the critical concentration for BPS formation, ϕ_{cr}. For these reasons the relatively small variations of the processing conditions may have a dramatic effect on morphology (e.g. high degree of co-continuity in blends mixed at 120 rpm for 45 min, but DPS morphology when mixed for additional 15 min). The full drawn line in Fig. 3 corresponds to the relation: $\phi_{i,\mathrm{HDPE}} = 5(\phi - 0.01)^{0.45}$. where the exponent value is ‘universal’ and the constant (5) was found by fitting the universal relation to experimental data [14]. The percolation theory predicted the value of exponent as 0.45. The derivation was carried out for spherical precursors, but empirically good fits have been found for other precursor shapes [4].

5. Discussion

The study demonstrates that blends with bi-continuous phase structure might be formed at very low volume fraction of the dispersed phase, $\phi_{\mathrm{cr}} > 0.001$. This would not be surprising if the mixing was carried our in extensional flow

Table 3
Observed morphologies for HDPE-3/PS-1 = 2.2 vol% blend

Shaft speed (rpm)	Mixing time (min)	Co-continuity index
5	15, 20, 30, 60	Low
20	15, 20, 30, 60	High
50	15, 20, 30, 60	High
80	15, 20, 30, 60	High
120	15	High
120	30	High
120	45	High
120	60	Zero
120	90	Zero
120	120	Zero

[5,6], but it is rather unprecedented for that in shear. Three approaches that may be used to explain the phenomenon are (in historical order):

1. The microrheological description of drops deformability and break in infinitely diluted Newtonian liquid mixtures.
2. The rheological theory of phase inversion in immiscible polymer blends.
3. The postulated in this work, the probabilistic in nature, relative rate of shear coalescence of dispersed drops vs. their break-up.

(1) The microrheology describes deformation of a single drop in a matrix (infinite dilution), thus it is unable to predict concentration-related effects. However, this well researched approach offers an excellent guidance how the individual drops are affected by external variables. The derived relations are valid at infinite dilution, but incorporation of a dynamic coalescence model had extended their applicability to blends comprising at least 10 vol% of the dispersed phase [28].

The microrheology states that co-deformation (that even for Newtonian system leads to formation of co-continuous structure) is expected at high value of the capillarity ratio, $\kappa^* > 2$, thus co-continuity is favored by high deforming stress, large particle size and low interfacial tension coefficient. Furthermore, the phase co-continuity is more likely to take place when the viscosity of the minor phase is higher than that of the matrix, $1 < \lambda^* < 3.8$. Within this range of λ^* a dynamic process determines the morphology, as the theory predicts breaking of the elongated drop when the shearing time exceeds the critical value $\theta^* > \theta_b^* = 99.31(\lambda^*)^{0.355}$. Thus, for $1 < \lambda^* < 3.8$ fibrillation and break-up is expected when the κ^* and θ^* parameters reach appropriate values. However, on a practical side, one should not expect that deformation of a single drop into a fiber would continue indefinitely. The stretching must reach a limiting fiber diameter—any further stretching will cause a break. For example when dilute PE/PS blends were prepared in a twin-screw extruder, the fiber diameter $d_{\mathrm{fiber}} > 0.1$ μm was observed. Evidently, the limiting diameter depends on the type of flow field.

The microrheology can be used to explain the observed co-continuity index for the HDPE-3/PS-1 blends reported in Table 3. At low mixing speeds and short times there is insufficient deformation of spherical drops to cause fibrillation hence the index is low. As the mixing speed and time increases there is increasing amount of deformation that result in formation of co-continuous structures. The process of stretching the HDPE-3 fibers continues until a critical value of θ^* is reached. The reduced blending time can be calculated from the relation: $\theta^* = \theta\dot{\gamma}\nu/\sigma_{12}\mathrm{d} \cong \theta[\nu/\mathrm{d}\eta(\dot{\gamma})]$. At 120 rpm the average rate of shear is $\dot{\gamma} \cong 100\ \mathrm{s}^{-1}$, and at that rate the matrix viscosity $\eta \cong 1$ kPa s. The value of the PS/PE interfacial tension coefficient was determined as $\nu = 6.4$ mN/m [29]. Assuming that the critical mixing time is 50 min and that the critical value of the reduced mixing time is the same for Newtonian and viscoelastic mixtures, $\theta_b^* = 99.31(\lambda^*)^{0.355} \simeq 162$, the fiber diameter at break $d = 0.13$ μm was calculated. Blending in an internal mixer is far removed from the smooth stretching of drop in Couette geometry, where from the relation for θ_b^* comes from. Surprisingly, in the case of HDPE-3 blended with PS-1 at $\phi_{\mathrm{cr}} = 0.014$, the fiber diameter at break was determined as $d \cong 0.1–0.2$ μm, which brackets the calculated value.

It is also important to consider the case of high viscosity ratios, $\lambda^* > 3.8$. Here, under strictly shear flow the drop might deform but not break (but breaking may take place in extensional flow). The theory predicts that the major axis of the deformed (prolate) drop is aligned in the flow direction. The degree of deformation depends of the level of stress transferred to the drop. Thus, within the limiting range viscosity ratios, $\lambda^* > 3.8$, fibrillation is possible by stretching the pre-existing drops either in shear or in extensional flow field, provided that stress is sufficiently large and the time of deformation sufficiently long.

(2) The rheological theory of phase inversion assumes that, independently of the viscosity ratio, the emulsion viscosity increases with concentration of the dispersed phase. The derived Eq. (1) implies that the critical volume fraction for the phase inversion must satisfy the inequality: $\theta_{\mathrm{perc}} \leq \theta_{2\mathrm{I}} \leq 1/2$, thus in 3D shear flow mixing $\phi_{2\mathrm{I}} \geq 0.156$ and in 1D extensional flow mixing $\theta_{2\mathrm{I}} \geq 0.019$. The derivation considers a single phase inversion concentration, not a range of compositions where phase co-continuity can be found because of the flow field heterogeneity, disparity between the break-up and coalescence rate or other reasons (e.g. related to the viscoelastic character of a given blend). The derived dependence compared well with the experimental mid-range concentrations for phase co-continuity.

The phase inversion theory suggests that to engender co-continuity of phases at low concentration extensional flow component during mixing should be maximized. Under the extensional flow the phase inversion at $0.019 \leq \phi_{\mathrm{cr}} \leq 0.156$ may be expected. However, since the experimental values of θ_{cr} listed in Table 4 are as low as about 0.001, the rheological theory of phase inversion cannot be used to describe the observation. Evidently, there is another mechanism responsible for co-continuity at such low concentrations.

(3) The hypothesis presented in this paper assumes that a critical condition for the phase co-continuity is that the rates of coalescence and of break-up are the same: $\theta_c = \theta_b$. When this condition is not met, at sufficient time available, the blends will either form well dispersed system or coalesce into two segregated phases. According to Eq. (8) a plot of $\log(\phi_{\mathrm{cr}}/\lambda\dot{\gamma})$ vs. $\log(\theta_b^*\lambda\dot{\gamma})$ should be a straight line with slope $-\mathrm{z}$ and intercept $\log k$. This indeed can be seen in Fig. 5.

The experimental values of ϕ_{cr} and the viscosity ratio, λ^*, are listed in Table 4. The other required variables were

Table 4
Critical co-continuity composition for A/B and B/A polymer blends

Polymer A	Polymer B	$\phi_{\mathrm{cr,A}}$	$\phi_{\mathrm{cr,B}}$	$(\eta_A/\eta_B)^a$	$\eta_{0,A}$ (kPa s)	$\eta_{0,B}$ (kPa s)	$(\eta_B/\eta_A)^a$	$\lambda\dot{\gamma}$ for B-phase
PS-1	PMMA	0.07–0.08	0.16–0.24	0.035	30	220	40	23
HDPE-3	PS-1	0.01	0.15–0.20	4	110	30	0.2	15
HDPE-3	PDMS-2	0.25	[b]	36	110	2.45		0.4
HDPE-4	PDMS-2	~0.25	[b]	~1	2.7	2.45	~1	0.4
HDPE-3	PMMA	~0.01	[c]	0.1	110	220	10	23
HDPE-3	PS-2	0.001[d]		~1	110	300		164

For PS-1/HDPE-3 blends where HDPE-3 constitutes the major phase: $\lambda\dot{\gamma} = 14$.

[a] Viscosity ratio at constant stress at $T = 180$ °C. The stress value was estimated as: $\sigma_{12} \simeq \dot{\gamma}\eta(\dot{\gamma})$, where $\dot{\gamma} \cong 20\ \mathrm{s}^{-1}$ and $\eta(\dot{\gamma})$ is the shear viscosity of the major phase resin.

[b] PDMS are fluids at room temperature and $\phi_{\mathrm{cr,B}}$ could not have been estimated by extraction.

[c] Depends on cooling rate (poor reproducibility).

[d] Difficult to get exact value. Evaluations: $0.001 \leq \phi_{\mathrm{cr}} < 0.005$. The lowest estimate is used in Fig. 5 since the experimental procedure gives values that are ≥ of the estimates because swelling pressure tends to destroy week networks.

calculated as follows:

- The relation between θ_b^* and $\lambda^* = \eta_D/\eta_C$ was estimated from Fig. 2 in Ref. [27]. For $\lambda^* \geq 4$ the value of θ_b^* is not defined by microrheology. Consequently the results for blends with $\lambda^* \gg 4$ are not included in Fig. 5. Experimentally, for different blends of this type $\phi_{\mathrm{cr}} = 0.15$–$0.30$ was observed [3,13,14,26].
- The relaxation time was calculated as $\lambda = \eta_0 H M_c/\rho RT$, where η_0 is the zero shear viscosity of the continuous phase, ρ is the density of the continuous phase, R is the gas constant, T is absolute temperature, the polydispersity ratio is $H = \bar{M}_w/\bar{M}_n$, and the critical molecular weight is twice as large as the entanglement molecular weight $M_c = 2M_e$.

As Fig. 5 shows, the experimental data for the blends with viscosity ratios: $\lambda^* \leq 4$ follow the predicted dependence with the exponent, $z = 2.01$, and the equation constant, $k = 1801$. The correlation coefficient is $r = 0.981$.

Thus the estimated correlation for the internal mixer is:

$$\phi_{\mathrm{cr}} = 1801/[(\theta_b^*)^{2.01}(\lambda\dot{\gamma})^{1.01}]$$

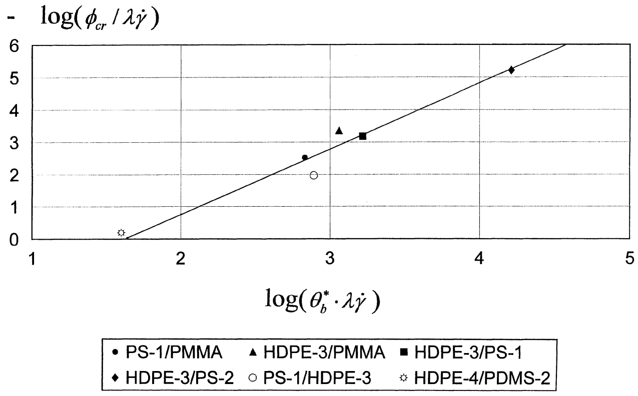

Fig. 5. $-\log(\phi_{\mathrm{cr}}/\lambda\dot{\gamma})$ vs. $\log(\theta_b^*\lambda\dot{\gamma})$ for data from Table 4 and viscosity ratio: $\lambda^* < 4$. Experimentally: $0.4 \leq (\lambda\dot{\gamma}) \leq 164$.

This equation should be treated as an approximation because:

- It builds on relatively few observations,
- It is based on a number of simplifying assumptions, e.g. application of a drop break up theory, which is valid at infinite dilution, and the assumption of a constant capillarity number for the viscosity ratios less than 4.

However, these simplifying assumptions are making Eq. (8) easy to use for predicting the conditions for co-continuity of phases. Furthermore, the relation does not contain difficult to measure morphological characteristics of the blend (e.g. fiber diameter). Hopefully, the equation will be a useful guide for the development of polymer blends with low critical volume fraction. Unfortunately, the two equation parameters are affected by the flow field, thus are not universal, but depend on the mixing equipment.

The present hypothesis resulted in Eq. (8), which predicts that ϕ_{cr} is inversely proportional to Deborah number raised to exponent $(z - 1)$, and to the reduced time-to-break, θ_b^*, raised to an exponent z. Since θ_b^* depends only on the viscosity ratio and the Deborah number depends on the shear rate, Eq. (8) should be used within the experimentally verified limit of variables, $0.4 \leq (\lambda\dot{\gamma}) \leq 164$.

6. Conclusions

An expression (Eq. (8)) giving a relation between critical volume fraction for BPS formation, a Deborah number, and a dimensionless break-up time is found to be well followed by the experimental data from internal mixer experiments. Application of the developed expression to processing/mixing equipment necessitates the estimation of the exponent z, and the equation parameter k.

Acknowledgements

The financial support of the Technical Science Council of Denmark is gratefully acknowledged.

References

[1] Utracki LA. Polymer alloys and blends. New York: Hanser Publishers; 1989.

[2] Sperling LH, Hu R. Interpenetrating polymer networks. In: Utracki LA, editor. Polymer blends handbook. Dordrecht: Kluwer Academic; 2002. Chapter 6.

[3] Stauffer D. Introduction to percolation theory, 2nd ed. London: Taylor & Francis; 1992.

[4] Lyngaae-Jørgensen J, Kuta A, Søndergaard K, Venø Poulsen K. Polym Networks Blends 1993;3:1.

[5] Starita JM. An Investigation of Polyethylene/Polystyrene Alloys. M. Engng Thesis. Princeton University; 1967.

[6] Thornton B, Villasenor RG, Maxwell B. J Appl Polym Sci 1980;25:653.

[7] Fayt R, Jerome R, Teyssié Ph. Makromol Chem 1986;187:837.

[8] Harrab C, Blacher S, Fayt R, Jerome R, Teyssié Ph. J Polym Sci, Part B: Polym Phys 1995;33:801.

[9] Mekhilef N, Verhoogt H. Polymer 1996;37:4069.

[10] Bourry D, Favis BD. SPE Technol Pap 1995;53:2001.

[11] Yang L-Y, Bigio D, Smith TG. SPE Technol Pap 1995;53:2010.

[12] Bogdanov B, Mikhailov M, Ilieva I. Acta Polym 1991;42:253.

[13] Vaughan AS. Polymer 1992;33:2513.

[14] Lyngaae-Jørgensen J, Utracki LA. Makromol Chem, Macromol Symp 1991;48/49:189.

[15] Lyngaae-Jørgensen J, Lunde Rasmussen K, Chtcherbakova EA, Utracki LA. Polym Engng Sci 1999;39:1060.

[16] Willemse RC, Posthuma de Boer A, van Dam J, Gotsis AD. Polymer 1999;40:827–34.

[17] Willemse RC, Posthuma de Boer A, van Dam J, Gotsis AD. Polymer 1999;39:5879–87.

[18] Veenstra H, van Dam J, Posthuma de Boer A. Polymer 1999;40:1119–30.

[19] Bourry D, Favis BD. J Polym Sci, Part B: Polym Phys 1998;36:1889–99.

[20] Utracki LA. J Rheol 1991;35:1615.

[21] Steinmann S, Gronski W, Friedrich C. Polymer 2001;42:6619–29.

[22] Oldroyd JC. Proc Roy Soc 1953;A218:122.

[23] Oldroyd JC. Proc Roy Soc 1955;A232:567.

[24] Veenstra H, Norder V, van Dam J, Posthuma de Boer A. Polymer 1999;40:5223–6.

[25] Elmendorp JJ. A Study of Polymer Blending Microrheology. PhD Thesis. University of Delft; 1986.

[26] Utracki LA. The rheology of multiphase systems. In: Covas JA, Agassant JF, Diogo AC, Vlachopoulos J, Walters K, editors. Rheological fundamentals of polymer processing. Dordrecht: Kluwer Academic; 1995. p. 113–37.

[27] Lyngaae-Jørgensen J. J Int Polym Proc 1999;14:213–20.

[28] Utracki LA, Shi GZH. Compounding polymer blends. Polymer blends handbook. Dordrecht: Kluwer Academic; 2002. Chapter 10.

[29] Luciani A, Champagne MF, Utracki LA. Makromol Chem, Macromol Symp 1998;126:307.